

Influence of temperature and surfactant on the photocatalytic performance of TiO₂ Nanoparticles

Ommeaymen Sheikhnejad-Bishe¹, Feng Zhao¹, Ali Rajabtabar-Darvishi¹, Erfan Khodadad², Ali Mostofizadeh¹ and Yudong Huang^{1,*}

¹Department of Polymer Science and Engineering, School of Chemical Engineering and Technology, Harbin Institute of Technology, Harbin 150001, People's Republic of China

²Surface Engineering Laboratory, School of Materials Science and Engineering, Dalian University of Technology, Dalian 116024, People's Republic of China

*E-mail: yduang.hit1@aliyun.com

Received: 16 March 2014 / Accepted: 22 April 2014 / Published: 19 May 2014

Synthesis of TiO₂ nanoparticles were performed by hydrothermal and sol-gel methods under 150 °C and 50 °C, respectively. The characteristic of different samples derived from different methods are compared. The effect of various parameters like temperature and surfactant (cetyltrimethyl ammonium bromide and urea) has been carried out in order to attain optimized pore morphology, high crystallinity, and to find desired adsorption condition. With the temperature increasing and surfactant applying, the morphology changed from equiaxed shape (T1) to cubic (T2) and rectangular shape (T3), and the particle size, crystal size and pore size show an increasing trend. Under the low temperature, the prepared nanoparticles are closed to single crystal morphology, but the samples possess polycrystalline morphology after the temperature increasing and surfactant applying. The photocatalytic activity was examined by degradation of Methylene blue under Xenon lamp and compared with P25. We found that those high-temperature synthesized samples exhibit significantly higher photocatalytic activities than the sample synthesized under low temperature so that the raspberry-like sample with the highest particle size displays dramatically (prominently) better photocatalytic activity higher than P25. This study provides a simple and inexpensive way to prepare high active anatase TiO₂.

Keywords: Anatase TiO₂; Photocatalytic activity; Hydrothermal; Sol-gel; Methylene blue; Surfactant.

1. INTRODUCTION

Titanium dioxide (TiO₂) is an attractive semiconducting material that has been widely utilized in various fields, and has attracted tremendous interest due to its unique optical and electrical

properties, good chemical stability, high photoactivity, strong oxidizing power and low cost [1-4]. These characteristics have been applied it to control environmental pollution, photocatalysis, solar energy conversion and storage, photovoltaic cells, photonic crystals, molecular sensors, gas sensors, medical applications and cosmetics [5-8].

TiO₂ is a polymorphous compound which exists in three types of rutile, anatase and brookite. All the types have the octahedral structure, but the arrangements of octahedral units are different. Anatase TiO₂ is more stable and also shows a better photocatalytic activity than the rutile due to its wide-band gap [7, 9].-Various methods and techniques have been developed to synthesize TiO₂ nano crystals, including sol-gel method, chemical vapor decomposition, hydrothermal technique, and reversed micelle method [4, 10-12] .

Since photocatalytic activity of TiO₂ is directly related to its morphology [4], all the oxidation reactions and photocatalysis take place on the surface of TiO₂. Additionally, the degradation rate of organic materials depends on the amount of catalytic surface active sites, surface area of the catalyst, light utilization, and other structural properties [6]. Since the mentioned properties can be improved by tailoring the shape and dimensionality, [13] the size and shape control of this material is a very important factor for accessing to the most applications of this semiconductor oxide.

Although there are a variety of reports on different synthesization methods of TiO₂, however, a comparative study to emphasize the effects of the various methods on the properties of the samples has not been yet reported. Herein, we report the synthesis of anatase TiO₂ with different shapes by simple and inexpensive methods such as hydrothermal and sol-gel methods. The objective of this paper is to compare the properties of the products with each other. We also investigate the role of the temperature and surfactant in the morphology of the samples. The goal is to discuss on the relationship between TiO₂ structure, specific surface area and photocatalytic activity.

2. EXPERIMENTAL

2.1. Sample Preparation

Preparation of TiO₂ via sol-gel method: All chemicals were provided from Sinopham Chemical Reagent Co. Ltd., and used as they delivered without further purification. The typical procedures were described as follow:

0.1 ml nitric acid was added drop by drop into 17 ml ethanol under vigorous stirring. Then, 9.75 ml titanium isopropoxide was slowly added to the above solution and followed by stirring for 10 minutes. The resulting yellowish solution was added to 150 ml distilled water drop wise under magnetic stirring at room temperature, and kept under vigorous stirring for 30 minutes. Then it was heated in the oven at 50°C for 24h to complete the crystallization process. The resulting precipitates were washed with distilled water, and then were dried in freeze drying at -60 °C for 24 hours. Finally, the powder was collected and ground in the mortar and pestle to obtain the fine powder used for further studying.

Preparation of TiO₂ via hydrothermal method: The TiO₂ solution was prepared by the same procedure as sol-gel method. In this method, 1.5 g cetyltrimethyl ammonium bromide (CTAB) was added into 150 ml distilled water as surfactant and stirred for 15 minutes. Then the yellowish solution was added drop by drop to CTAB solution under stirring and also kept stirring for 30 minutes. After, different amounts of urea (surfactant) were added into the solution. The derived solution was transferred into the autoclave, which was heated at 150°C for 20h, and cooled to the room temperature naturally. The resulting white precipitates were washed with distilled water and dried in freeze drying for 24h.

2.2. Characterization

The phases of the products were determined by X-ray diffraction (XRD), performed on (RIGAK D/MAX-r-B). The average crystal size was determined by XRD peak broadening using the Scherrer equation:

$$t = \frac{K\lambda}{(\beta \cdot \cos \theta)} \quad (1)$$

Where t is the average crystal size, $K (= 0.89)$ is the Scherrer constant, $\lambda (= 0.15418 \text{ nm})$ is the X-ray Cu- K_{α} radiation wave length, β is the peak width of half maximum, and θ is the Bragg diffraction angle.

The morphologies of the products were studied by scanning electron microscopy (SEM, Hitachi S-3700) and transmission electron microscopy (TEM, Hitachi H-7650). The N₂ adsorption-desorption Brunauer-Emmett-Teller (BET) surface areas were determined by nitrogen adsorption method (ASAP2020, Micrometrics). The average particle size was measured by the following equation:

$$D = \frac{6000}{(\rho \cdot S_{\text{BET}})} \quad (2)$$

Where D was the average particles size, $\rho = 4.2 \text{ g/cm}^3$ was the density of TiO₂ and the S_{BET} was the specific surface area. The average particle size is estimated by assuming that the particles are spherical and they have a similar density.

2.3. Photocatalytic activity tests

The photocatalytic activity of the prepared TiO₂ was evaluated by degradation of Methylene blue (MB) under UV light irradiation at the ambient temperature. 0.06 g of TiO₂ was dispersed into 80 ml MB ($3 \times 10^{-5} \text{ M}$) aqueous solution. The mixture was put in ultrasonic for 10 minutes and it was kept in the dark area under stirring for 1h to ensure the establishment of an adsorption/desorption equilibrium. Then, the samples were illuminated with a 150W Xenon lamp source. Portions of approximately 6 ml solutions were taken at selected time intervals and centrifuged at 11000 rpm for 9 min. The remaining MB in the solution system was detected by a UV-752N PC spectrometer at a wavelength of 670 nm.

3. RESULTS AND DISCUSSION

3.1. Phase construction, Morphology and structures

Fig. 1 shows the XRD patterns of the products synthesized with different methods. The XRD patterns reveal the overall crystalline structure and phase purity of the nanostructures. The samples identification is summarized in Table 1.

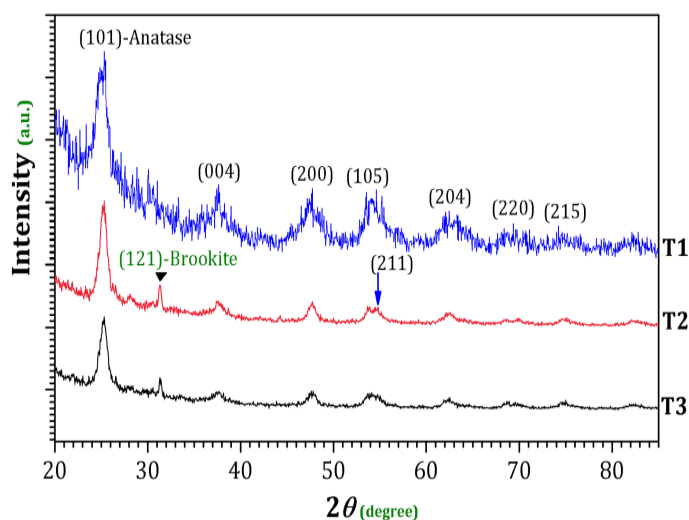


Figure 1. XRD patterns of TiO₂ samples prepared by different methods: T1-(Sol-gel), T2-(Hydrothermal, 0.1g Urea), and T3-(Hydrothermal, 0.2g Urea). Results displayed the characteristic peaks of anatase and the phase at 30.8° corresponds to brookite phase. The phase at 53.9° corresponds to triangular crystalline lattice (105).

Table 1. Preparation materials, methods and crystal structures of TiO₂ samples.

Sample number	Content			Method	Phase from XRD pattern
	Acid (ml)	CTAB (g)	Urea (g)		
T1	0.1	-	-	Sol-gel	Anatase
T2	0.1	1.5	0.1	Hydrothermal	Anatase+Brookite
T3	0.1	1.5	0.2	Hydrothermal	Anatase+Brookite

Sample T1 prepared via the sol-gel method under low temperature can be readily indexed to pure anatase phase, which is in agreement with the reported values of JCPDS No. 29-1360. For this sample, several weak peaks can be identified, indicating the slight crystallization of this sample. Despite the low temperature and the simple process for preparation of this sample, no characteristic peaks of other impurities are observed which indicates the high purity of the product [14]. For the samples T2 and T3 which derived from hydrothermal method under high temperature, most of the peaks belong to the anatase phase (JCPDS No. 21-1272), except for the slight peak at 30.8°, which corresponds to brookite (JCPDS No. 29-1360).

It indicates that these samples possess a mixed crystal phases. Strong peak can be clearly seen for these samples, indicating the high crystallization. The sharpness of the peaks implies the high crystallinity of the TiO_2 products. As shown in the XRD pattern, T2 has the sharpest peaks which indicates the best crystalline of the power via the hydrothermal method [15]. The XRD results indicate that the phases and rate of crystallinity of the products are highly sensitive to the method and the temperature.

Morphology and the particle size of the photocatalyst often play an important role in the catalytic properties by changing in light absorption and transmission [16]. The morphology and microstructures of the samples were investigated using SEM and TEM.

SEM images of the prepared samples via different methods are shown in Fig. 2. As it can be seen, nanoparticles are uniformly distributed throughout the samples with rough surface, and the particles sizes are fairly small. Under the low temperature in sol-gel method (Fig. 2a), the sample has an equiaxed shape with slight agglomeration. With increasing the temperature and surfactant addition in hydrothermal method (Fig. 2b and c), the samples possess well defined shape and larger particle size, which are due to using surfactant and higher temperature. Raspberry-like structures were observed in sample T2 (Fig. 2b).

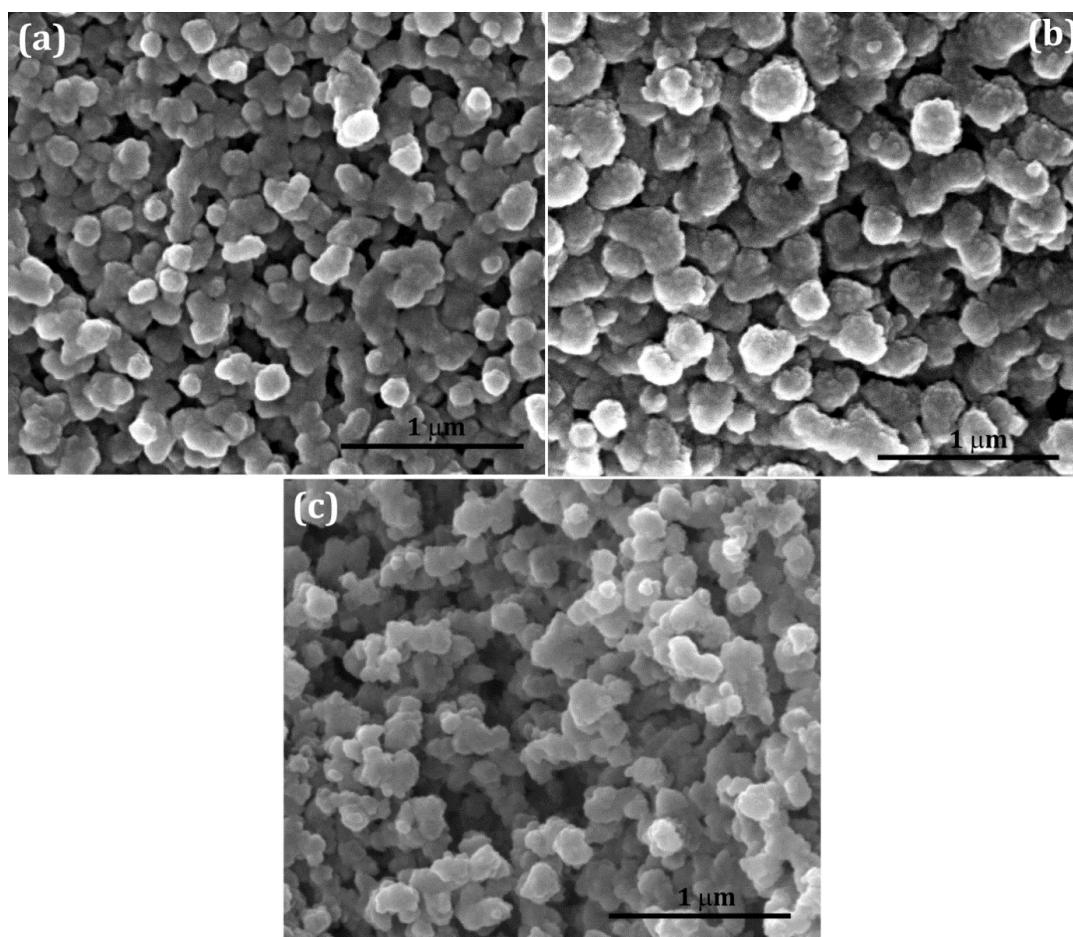


Figure 2. SEM images of as-prepared samples by different methods: (a) T1-(Sol-gel), (b) T2-(Hydrothermal, 0.1g Urea), and (c) T3-(Hydrothermal, 0.2g Urea).

These small particles connected to each other so that the size of an individual particle is hard to be estimated. The particle sizes also increased with an increase in temperature via hydrothermal method. As an interesting result, temperature plays an important role in the structure and morphology of the products during the synthesis processes [17-19].

In this study, TEM was used to obtain more information about the samples. Furthermore, the technique based on TEM provides adequate evidences to illustrate the morphology and the size of the samples. Fig. 3 shows TEM images of the samples. As can be observed in Fig. 3a, the TEM image of T1 reveals that the particles possessed equiaxed shapes but T2 and T3 particles take much more regular shape due to the temperature increasing via hydrothermal method which is in good agreement with SEM results. As shown in Fig. 3b and c, the TEM images display very good crystalline morphology of the particles with cubic and rectangular morphology, respectively.

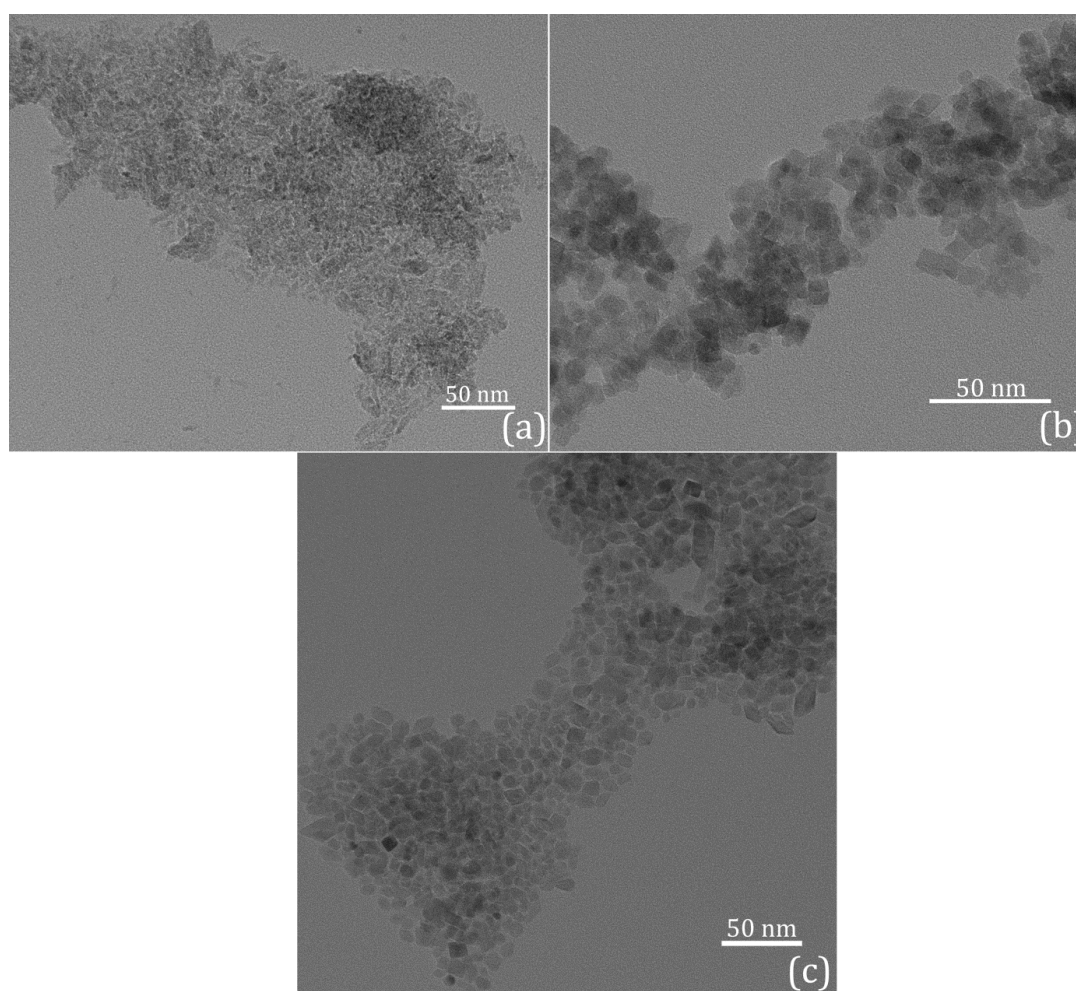


Figure 3. TEM images of TiO_2 samples prepared by different methods: (a) T1-(Sol-gel), (b) T2-(Hydrothermal, 0.1g Urea), and (c) T3-(Hydrothermal, 0.2g Urea).

Fig. 4 illustrates the variation of the crystal size and particle size of the samples which were calculated using Eq. (1) and (2), respectively [20, 21]. The particle size obtained by BET method shows a similar trend as the crystal size calculated from Scherrer's equation. The average particle size

and crystal size of T1 are very close to each other. This indicates that the prepared nanoparticles are closed to single crystal morphology. But T2 and T3 have crystal size significantly smaller than their particle size indicating polycrystalline morphology of the nanoparticles which caused by high temperature and surfactant. According to the results, the average particle size of T2 is larger than T3. It is obvious that after increasing the amount of urea, the cubic particles were coagulated together to make a secondary structure of rectangular shape. On the other hand, under high temperature, the crystallographic orientation wasn't completed to construct stable rectangular shapes which caused some small particles. Finally, the average particle size was decreased.

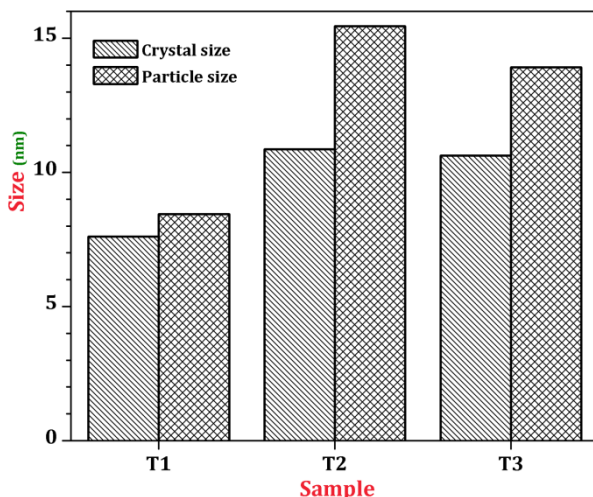


Figure 4. Crystal size and particle size of the as-prepared samples.

Fig. 5 shows the schematic illustration of the formation and the growth mechanism of TiO₂ nanoparticles prepared by different methods. It can be deduced that TiO₂ nanoparticles could have different morphology depends on outer chemical and physical conditions, including temperature and the amount of surfactant.

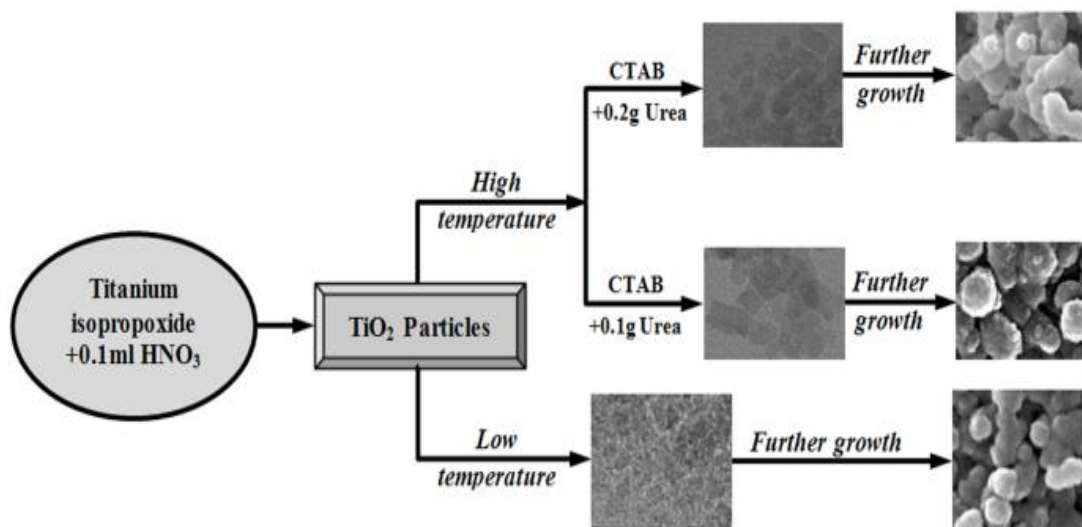


Figure 5. Schematic illustration of growth mechanism of TiO₂ formation.

3.2. N₂ adsorption-desorption analysis

The nitrogen adsorption–desorption isotherms of samples are shown in Fig. 6. The specific surface areas, pore sizes and pore volumes calculated by BET and Barret-Joyner-Halenda methods are listed in Table. 2.

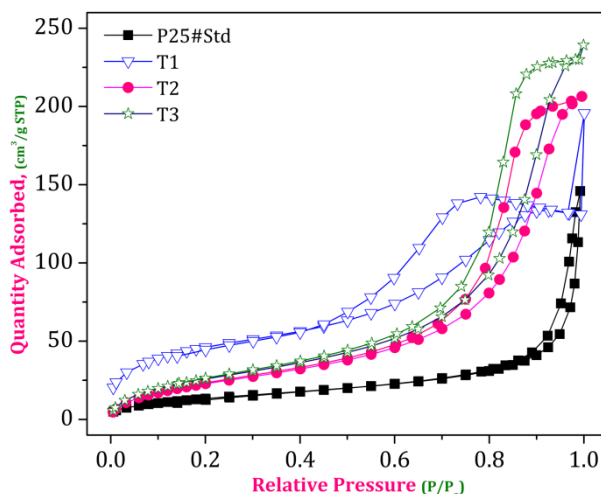


Figure 6. N₂ adsorption-desorption isotherm of as-prepared samples prepared by different methods: T1-(Sol-gel), T2-(Hydrothermal, 0.1g Urea), T3-(Hydrothermal, 0.2g Urea) and P25.

As seen from Fig. 6 and according to the IUPAC classification [22], the isotherms of TiO₂ samples are identified as IV-like isotherm type with a type of H2 hysteresis loop for T1 and H1 hysteresis loop for T2 and T3. This indicates that the synthesized samples have mesoporous structure. H1 hysteresis loop is extreme conditions but H2 hysteresis loop is the medium condition. The distribution of pore sizes and the pore shape in H2 type is not well-defined or irregular [22].

According to Table 2, specific surface areas of all samples are much higher than that of commercial TiO₂ nanoparticle (P25), which can provide more active catalytic sites [6]. This fact implies that the formation of the samples by these methods causes a significant increase on the surface area of TiO₂ particles [23]. According to the results, all the samples have mesoporous properties and T1 possess the smallest pore size. This was probably resulted from the further growth of the samples and also surfactant addition during the hydrothermal treatment which is in agreement with SEM and TEM results.

Table 2. Textural properties of different TiO₂.

Sample	BET surface area (m ² .g ⁻¹)	Average pore diameter (Å)	Total pore volume (cm ³ .g ⁻¹)
P25	51.37	86.27	0.110
T1	169.37	47.85	0.202
T2	92.45	134.89	0.311
T3	102.72	138.47	0.355

3.3. Photocatalytic activity

Photocatalytic activities of the samples are evaluated by the degradation of MB in aqueous solution under UV light irradiation. Temporal changes in the concentration of MB are monitored by examining the variations in UV-visible spectra at 670 nm.

Fig. 7 presents the concentration changes of MB with irradiation time for the samples T1, T2, T3 and P25. As presented in Fig. 7, the concentration of the dye solutions decreased with prolonged irradiation time while the order of photocatalytic activity was $T2 > P25 > T3 > T1$.

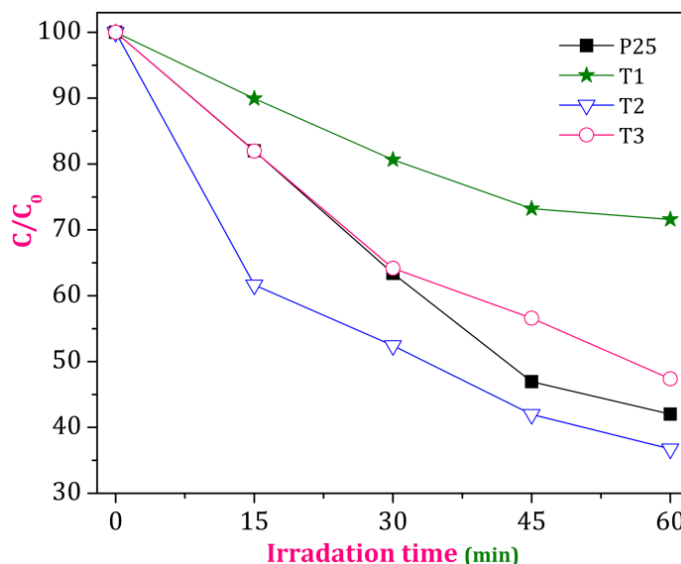


Figure 7. Photocatalytic degradation of Methylene blue by different photocatalysts and methods: T1-(Sol-gel), T2-(Hydrothermal, 0.1g Urea), T3-(Hydrothermal, 0.2g Urea) and P25 during the irradiation time.

Anatase is reported to be the active phase in the photocatalytic reaction [24], probably because the anatase phase contains more amounts of oxygen vacancy sites contributing to the performance of the catalytic oxidation process [25]. It is accepted that photoactivity of TiO_2 depends on the morphology, crystallization of the sample and surface area of the photocatalysts [2, 9, 23, 26, 27]. According to these results, the samples which prepared via the hydrothermal method have better crystallization, which promoted the photocatalytic activity of samples. Despite T1 has the highest surface area and the smallest particle size, the photocatalytic activity of this sample is the lowest one. However, the imperfect crystallization from XRD spectra (Fig. 1) accompanying with the irregular structure which resulted in the decreasing of degradation of the pollutant. The photocatalytic activity of T2 and T3 are better than T1. At the beginning of the irradiation time, the photocatalytic activity of T3 was also as well as P25, but the photocatalytic performance of the sample was slightly degenerated by prolonging the irradiation time due to the high agglomeration of this sample. The photocatalytic activity of raspberry-like specimen is superior of P25. The increase of photocatalytic activity can be explained considering two factors. First, raspberry-like sample has a larger surface area than P25. Such

adequate area provides further active sites for photodegradation reactions. Second, the raspberry shape structures possess a good crystallinity making them promising candidate for degradation of the pollutant. The results revealed that the use of raspberry like TiO₂ with unique structure could accelerate the photocatalytic activity.

4. CONCLUSION

In this work, we have reported the synthesis of anatase TiO₂ via sol-gel and hydrothermal reaction condition. The structure, specific surface area and photocatalytic activities of the resulting samples were investigated. The results demonstrated that all the as-prepared samples have higher specific surface area than P25. Sample T2 with raspberry shape possess good crystallinity, exhibiting high photocatalytic activity and photodegradation of organic pollutants while sample T1 has the worst photocatalytic activity. On the other hand, the properties of the samples prepared by the hydrothermal method are extremely better than the other sample. This effect illustrated that synthesis temperature exerts a great influence on the morphology, structure and properties of the samples. T2 also exhibited higher photocatalytic activity than P25 which owing to the combined effects of both the structural characteristic and the specific surface area. Based on this study, we inferred that good crystallinity, high specific surface area, and the morphology correlate with the photocatalytic efficiencies. As technical advantages, this study provides a simple and inexpensive way to prepare high active anatase photocatalyst. This material may be attractive in the field of photocatalysis and surface modification of TiO₂ for higher efficiency photocatalysts.

ACKNOWLEDGEMENT

The authors gracefully acknowledge supports from the Changjiang scholars program and the national Nature science foundation of China (No. 51073047 and No. 91076015).

References

1. Y.-C. Hsu, H.-C. Lin, C.-H. Chen, Y.-T. Liao, and C.-M. Yang, *J. Solid State Chem.*, 183 (2010) 1917.
2. J. Li, C.-J. Lin, Y.-K. Lai, and R.-G. Du, *Surf. Coat. Technol.*, 205 (2010) 557.
3. Z. Sun, J. H. Kim, Y. Zhao, F. Bijarbooneh, V. Malgras, Y. Lee, Y.-M. Kang, and S. X. Dou, *JACS*, 133 (2011) 19314.
4. X. H. Xia, Y. Liang, Z. Wang, J. Fan, Y. S. Luo, and Z. J. Jia, *Mater. Res. Bull.*, 43 (2008) 2187.
5. G. Wu, J. Wang, D. F. Thomas, and A. Chen, *Langmuir*, 24 (2008) 3503.
6. G. Tian, Y. Chen, W. Zhou, K. Pan, C. Tian, X.-r. Huang, and H. Fu, *CrystEngComm*, 13 (2011) 2994.
7. L. Zhang, Q. Ding, and Y. Zhou, *Cryst. Res. Technol.*, 46 (2011) 1202.
8. X. Shen, J. Zhang, and B. Tian, *J. Mater. Sci.*, 47 (2012) 3855.
9. Y. Wang, L. Zhang, K. Deng, X. Chen, and Z. Zou, *J. Phys. Chem. C*, 111 (2007) 2709.
10. J. Jitputti, T. Rattanavoravipa, S. Chuangchote, S. Pavasupree, Y. Suzuki, and S. Yoshikawa, *Catal. Commun.*, 10 (2009) 378.

11. J. Liao, L. Shi, S. Yuan, Y. Zhao, and J. Fang, *J. Phys. Chem. C*, 113 (2009) 18778.
12. Y. Masuda, T. Ohji, and K. Kato, *Crystal Growth & Design*, 10 (2009)
13. H. WANG, Y. WANG, W. ZHAO, C. LIANG, Y. LIU, H. WANG, and H. LI, *Optoelectron. Adv. Mater. Rapid Commun.*, 4 (2010) 803.
14. H. Pan, J. Qian, Y. Cui, H. Xie, and X. Zhou, *J. Mater. Chem.*, 22 (2012) 6002.
15. X. Yin, W. Que, Y. Liao, H. Xie, and D. Fei, *Colloids Surf., A*, 410 (2012) 153.
16. N. Riaz, F. K. Chong, B. K. Dutta, Z. B. Man, M. S. Khan, and E. Nurlaela, *Chem. Eng. J.*, 185 (2012) 108.
17. R. Yoshida, Y. Suzuki, and S. Yoshikawa, *J. Solid State Chem.*, 178 (2005) 2179.
18. J. Yu, H. Yu, B. Cheng, and C. Trapalis, *J. Mol. Catal. A: Chem.*, 249 (2006) 135.
19. J. Jitputti, Y. Suzuki, and S. Yoshikawa, *Catal. Commun.*, 9 (2008) 1265.
20. M. A. Behnajady, N. Modirshahla, M. Shokri, H. Elham, and A. Zeininezhad, *J. Environ. Sci. Health., Part A*, 43 (2008) 460.
21. M. Huang, C. Xu, Z. Wu, Y. Huang, J. Lin, and J. Wu, *Dyes Pigments*, 77 (2008) 327.
22. W. Qing, J. Guojun, L. Hongpeng, B. Jingru, and L. Shaohua, *Oil Shale*, 27 (2010) 135.
23. C. Guo, J. Xu, Y. He, Y. Zhang, and Y. Wang, *Appl. Surf. Sci.*, 257 (2011) 3798.
24. Z. Ding, G. Lu, and P. Greenfield, *J. Phys. Chem. B*, 104 (2000) 4815.
25. S. Song, Z. Liu, Z. He, A. Zhang, J. Chen, Y. Yang, and X. Xu, *Environ. Sci. Technol.*, 44 (2010) 3913.
26. P. Xinyan and D. Enyong, *Micro. Nano. Lett.*, 6 (2011) 998.
27. K. Liu, L. Zhu, N. Li, Y. Sun, H. Li, and X. Zhu, *Cryst. Res. Technol.*, 47 (2012) 1088.

© 2014 The Authors. Published by ESG (www.electrochemsci.org). This article is an open access article distributed under the terms and conditions of the Creative Commons Attribution license (<http://creativecommons.org/licenses/by/4.0/>).